Unique Binding of Nitric Oxide to Ferric Nitric Oxide Reductase from *Fusarium oxysporum* Elucidated with Infrared, Resonance Raman, and X-ray Absorption Spectroscopies

Eiji Obayashi,[†] Koki Tsukamoto,[‡] Shin-ichi Adachi,[§] Satoshi Takahashi,[§,||] Masaharu Nomura,[⊥] Tetsutaro Iizuka,[§] Hirofumi Shoun,[▽] and Yoshitsugu Shiro*[,§]

Contribution from them Department of Applied Chemistry, Chuo University, Bunkyo-ku, Tokyo 112, Japan, College of Science and Technology, Nihon University, Chiyoda-ku, Tokyo 101, Japan, The Institute of Physical and Chemical Research (RIKEN), Hirosawa 2-1, Wako, Saitama 351-01, Japan, Photon Factory, National Laboratory for High Energy Physics, Tsukuba, Ibaraki 305, Japan, and Institute of Applied Biochemistry, University of Tsukuba, Tsukuba, Ibaraki 305, Japan

Received October 30, 1996. Revised Manuscript Received April 9, 1997[⊗]

Abstract: Nitric oxide reductase from the denitrifying fungus *Fusarium oxysporum* catalyzes the reduction of NO to N_2O [Nakahara, K., et al. *J. Biol. Chem.* **1993**, *268*, 8350−8355]. Since this enzyme belongs to the cytochrome P450 superfamily [Kizawa, H., et al. *J. Biol. Chem.* **1991**, *266*, 10632−10637], it is called cytochrome P450nor (P450nor), but does not exhibit monooxygenation activity. In the present study, we examine the coordination structure of the heme iron in P450nor in the ferric-NO form by using infrared, resonance Raman, and X-ray absorption (EXAFS = extended X-ray absorption fine structure) spectroscopies, since the ferric-NO complex is a first intermediate in the NO reduction cycle by P450nor [Shiro, Y, et al *J. Biol. Chem.* **1995**, *270*, 1617−1623]. We compared the data obtained with those for the *d*-camphor-bound form of *Pseudomonas putida* camphor hydroxylase cytochrome P450cam (P450cam), a typical model of the monooxygenase. From the vibrational spectroscopic measurements, we found that the Fe-bound N−O stretching frequency (ν(N−O)) occurred at 1851 cm^{-1} and the Fe−NO stretching frequency (ν(Fe−NO)) at 530 cm^{-1} for P450nor, while those at 1806 and 522 cm^{-1} were observed for P450cam, respectively. The assignments were confirmed by the ^{15}NO substituting effect on these vibrational frequencies. These results indicated that NO binds to the ferric iron in P450nor stronger than in P450cam. Support for this was provided from the EXAFS study, which gave an $Fe-N_{NO}$ bond distance of 1.66 ± 0.02 Å for P450nor and 1.76 ± 0.02 Å for P450cam. These spectroscopic results suggest that, compared with P450cam, the lower steric hindrance and/or the difference in the electrostatic interactions of the ligand NO with its surroundings facilitates the donation of the NO 2pπ* electron to the iron 3dπ orbital, resulting in the strengthening of the Fe−NO and the N−O bonds of P450nor. The vibrational spectral observation of the ferrous-CO complex of P450nor supported this suggestion. This configuration can reduce the electron density on the NO ligand in P450nor, which is seemingly relevant to the NO reduction reactivity of P450nor.

Introduction

Nitric oxide reductase (NOR) isolated from the fungus *Fusarium oxysporum* is involved in the fungal denitrification process and catalyzes the reduction of NO to N_2O according to the following reaction scheme.[1]

$$2NO + NADH + H^+ \rightarrow N_2O + NAD^+ + H_2O$$

The turnover number of this catalytic reaction was determined to be more than 1000 s^{-1} at 10 °C, suggesting a very effective NO diminishing system. Biochemical studies have shown that the molecular weight of the *F. oxysporum* NOR is about 46 000 and that the enzyme contains one protoheme (iron−protoporphyrin complex) as a prosthetic group.[1,2] Optical and EPR spectral properties demonstrated the coordination of the thiolate anion from Cys as a fifth axial ligand, which is the common structural unit of cytochrome P450 (P450).[2] Furthermore, the amino acid sequence of the *F. oxysporum* NOR has up to 40% homology with other P450s, as was revealed by the DNA sequence analysis.[1c] The *F. oxysporum* NOR has been classified into the P450 superfamily and is specifically designated cytochrome P450nor (P450nor).[1c]

However, the biological function of P450nor is unique, compared with other usual P450s. While the usual P450s are involved in the metabolism of many biological substances via the monooxygenation reaction using O_2,[3] P450nor can catalyze the NO reduction but not the monooxygenation.[1e,2c] It is reasonable to suggest that some subtle but significant differences

* Author to whom correspondence should be addressed.
[†] Chuo University.
[‡] Nihon University.
[§] RIKEN.
[||] Present address: Department of Molecular Engineering, Graduate School of Engineering, Kyoto University, Kyoto 606-01, Japan.
[⊥] National Laboratory for High Energy Physics.
[▽] University of Tsukuba.
[⊗] Abstract published in *Advance ACS Abstracts,* August 1, 1997.

(1) (a) Shoun, H.; Sudo, Y.; Seto, Y.; Beppu, T. *J. Biochem.* **1983**, *94*, 1219−1229. (b) Shoun, H.; Suyama, W.; Yasui, T. *FEBS Lett.* **1989**, *244*, 11−14. (c) Kizawa, H.; Tomura, D.; Oda, M.; Fukamizu, A.; Hoshino, T.; Gotoh, O.; Yasui, T.; Shoun, H. *Ibid.* **1991**, *266*, 10632−10637. (d) Shoun, H.; Tanimoto, T. *Ibid.* **1991**, *266*, 11078−11082. (e) Nakahara, K.; Tanimoto, T.; Hatano, H.; Usuda, K.; Shoun, H. *J. Biol. Chem.* **1993**, *268*, 8350−8355.

(2) (a) Shiro, Y.; Kato, M.; Iizuka, T.; Nakahara, K.; Shoun, H. *Biochemistry* **1994**, *33*, 8673−8677. (b) Nakahara, K.; Shoun, H.; Adachi, S.; Iizuka, T.; Shiro, Y. *J. Mol. Biol.* **1994**, *239*, 158−159. (c) Shiro, Y.; Fujii, M.; Iizuka, T.; Adachi, S.; Tsukamoto, K.; Nakahara, K.; Shoun, H. *J. Biol. Chem.* **1995**, *270*, 1617−1623. (d) Shiro, Y.; Fujii, M.; Isogai, Y.; Adachi, S.; Iizuka, T.; Obayashi, E.; Makino, R.; Nakahara, K.; Shoun, H. *Biochemistry* **1995**, *34*, 9052−9058.

S0002-7863(96)03781-X CCC: $14.00

in the structure at the active site are responsible for the difference in the biological properties between P450nor and usual P450s. This difference should be reflected in the redox potential of P450nor in the Fe^{3+}/Fe^{2+} couple (−307 mV), which is significantly lower than the value observed for the *d*-camphor-bound form (−140 mV) of *Pseudomonas putida* cytochrome P450cam (P450cam).[2d] The results suggested that the iron coordination structure and/or the electrostatic interaction between the heme and its surroundings substantially differs between P450nor and P450cam, because both of these factors have been considered to be important in regulating the iron redox properties of hemoproteins. To study the iron coordination structure of P450nor, we also examined the EPR spectra of P450nor in the ferric-CN^- and ferrous-NO states. However, their EPR spectral features were basically the same as those of P450cam,[2d] indicating that the coordination structures of the iron at least in these states are quite similar between P450nor and P450cam.

We kinetically and spectrophotometrically followed the reaction of P450nor with NO and NADH and proposed the molecular mechanism of the NO reduction catalyzed by P450nor on the basis of these results.[2c] In this mechanism, NO binds to the ferric enzyme to yield its ferric-NO complex, and the resultant complex can accept two electrons transferred directly from NADH to reduce NO and then to produce N_2O through a transient formation of the characteristic intermediate **I**. The ferric-NO complex of P450nor is, thus, a first intermediate in the NO reduction reaction. It is also worth noting that the ferric NO complex of P450cam is inactive to the NO reduction. These observations led us to characterize the coordination and electronic structures of the ferric-NO complex of P450nor and to compare them with those of P450cam, using several spectroscopic methods such as infrared (IR), resonance Raman, and X-ray absorption (EXAFS = extended X-ray absorption fine structure) spectroscopies. In the present study, we found that the NO coordination to the ferric iron in P450nor is specifically different from that in P450cam and that the difference is relevant to the difference in the functional properties between P450nor and P450cam.

Materials and Methods

Enzymes. Cytochrome P450nor was isolated from the denitrifying cells of *F. oxysporum* according to a previously described procedure[1a,e] and purified using DEAE-cellulose (DE-52, Whatman, U.K.) and Sephadex G-100 (Pharmacia, Sweden) column chromatographies. The sample was dissolved in 20 mM potassium phosphate buffer, at pH 7.2, containing 10% glycerol, 0.1 mM dithiothreitol, and 0.1 mM EDTA. We used cytochrome P450cam expressed and purified from *Escherichia coli* strain JM109 containing the P450cam expression system. The cell growth and the isolation and purification of the protein have been previously described.[4] It was shown that the spectroscopic and enzymatic properties of the wild-type P450cam expressed in *E. coli* are identical to those of P450cam from *Pseudomonas putida*. The *E. coli* transformed with plasmid pUC19 carrying a gene for the wild-type enzyme was a generous gift from Profs. Y. Ishimura and H. Shimada of Keio University.

Infrared Spectral Measurement. The infrared spectra were measured using a JEOL JIR600 spectrometer with a resolution of 4 cm^{-1} at room temperature. The sample, whose concentration was 2−3 mM, was transferred into the IR cell having CaF_2 windows with a path length of 0.050 mm under anaerobic conditions. To obtain the final spectrum, 100 interferograms were accumulated and then Fourier transformed. ^{15}NO gas was purchased from Shoko Co. Ltd. (Tokyo).

Resonance Raman Measurements. The resonance Raman spectra were measured with a JASCO NR-1800 spectrometer modified in a single dispersion mode equipped with a liquid-nitrogen-cooled CCD detector (Princeton Instruments). The slit width for the spectral measurements was 5 cm^{-1}. The excitation wavelengths used for the measurements were 413 nm from a Krypton ion laser (Coherent, Innova90) and 441 nm from a He-Cd vapor laser (Kimmon Elect. Co. Ltd., Saitama, Japan). The power of the Kr^+ and He-Cd lasers at the sample were about 10 and 4 mW, respectively. Holographic filters (Kaiser Optical Systems, Inc.) were used to remove the Rayleigh scattering. The cylindrical Raman cell containing the sample solution, whose concentration was 40 μM, was spun to minimize local heating and photodissociation of the iron-bound NO and CO and was cooled (∼20 °C) under flowing prechilled dry nitrogen gas. To obtain the final spectrum, a total of 30 spectra, each acquired for 1 min, were averaged. Calibration of the Raman spectrophotometer was carried out using indene and potassium hexacyanoferrate(II) as standards.

EXAFS Measurements. All of the EXAFS spectra were recorded using monochromatized synchrotron radiation at BL-12C of the Photon Factory of the National Laboratory for High Energy Physics (Tsukuba, Japan). The concentration of the samples for EXAFS measurements was 1−2 mM, and the samples were frozen in liquid nitrogen. The EXAFS spectra were recorded at 80 K as a fluorescence excitation spectra using a bent-cylinder-type focusing mirror and a silicon(111) double-crystal monochromator. The sample was placed at a 45° angle against the incident X-ray beam, and the fluorescent X-ray intensity perpendicular to the beam was measured using a solid state detector (SSD) with a 19-element (Canberra Industries, Inc). At 2.5 GeV and 320 mA, the count rate from the SSD was about 8000 cps. The spectrum presented represents the average of a 8−10 h scan.

The analysis of the EXAFS data was performed using the programs EXCURV92[5] and SPLINE.[6] (SPLINE is a program to extract XAFS from raw X-ray absorption data programmed by Ellis, P. J. (School of Chemistry, University of Sydney, 1995).) A polynomial fit to the pre-edge region (∼6800−7100 eV) and a cubic spline fit to the above-edge region were done interactively by the program SPLINE. EXCURV92 with the constrained and restrained refinement, in which multiple scattering paths to the third order involving angles of greater than 120° were included, was used to obtain the best simulation to our EXAFS data. In particular, the multiple scattering from the outershell atoms of the porphyrin ring and axial ligand molecules were taken into account. In constrained refinement, the number of parameters is reduced by treating a set of scattering atoms as a unit. In our case of the iron−porphyrin system axially coordinated by cysteine and a sixth ligand molecule, the structure of the porphyrin ring was idealized to give C_4 symmetry, and one-fourth of the ring, *i.e.*, the atoms of the pyrrole ring and the bridging *meso* carbon, was defined as unit 1, as shown in Figure 1A,B. In addition, the S_γ, C_β, and C_α atoms of cysteine residue were defined as unit 2, and the sixth ligand molecules (H_2O and NO), if any, were included as unit 3, as shown in Figure 1C,D. The numbering of atoms which is used in our refinement is also shown in Figure 1. Initial coordinates of atoms in unit 1 were derived from the crystal structure of bis(imidazole)(α,β,γ,δ-*meso*-tetraphenylporphinato)iron(III) chloride, and those in units 2 and 3 were derived from the crystal structure of ferric cytochrome P450cam and from crystal structure of ligand molecules coordinated to a iron atom, respectively. The coordination numbers for units 1, 2, and 3 are fixed as 4, 1, and 1, respectively, throughout the refinement. When each unit is defined, refinement of position and single angular parameter of one atom in each unit allows the position of the remaining atoms of the ligand to be simultaneously refined. The number of Debye−Waller parameters were also reduced by making the assumption that chemically similar

(3) (a) Ortiz de Montellano, P. R., Ed.; *Cytochrome P450, Structure, Mechanism, and Biochemistry,* 2nd ed.; Plenum Press: New York, 1995. (b) Schuster, I., Ed.; *Cytochrome P450*: *Biochemistry and Biophysics*; Taylor & Francis: Bristol, PA, 1989. (c) Sato, R., Omura, T., Eds.; *Cytochrome P450*; Academic Press: New York, 1978.

(4) Imai, M.; Shimada, H.; Watanabe, Y.; Matsushima-Hibiya, Y.; Makino, R.; Koga, H.; Horiuchi, T.; Ishimura, Y. *Proc. Natl. Acad. Sci. U.S.A.* **1989**, *86*, 7823−7827.

(5) (a) Strange, R. W. Blackbern, N. J.; Knowles, P. F.; Hasnain, S. S. *J. Am. Chem. Soc.* **1987**, *109*, 7157−7162. (b) Binsted, N.; Strange, R. W.; Hasnain, S. S. *Biochemistry* **1992**, *31*, 12117−12125. (c) Teo, B. K. *EXAFS: Basic Principles and Data Analysis;* Springer-Verlag: Berlin, 1986.

(6) Ellis, P. J.; Freeman H. C. *J. Synchrotron Rad.* **1995**, *2*, 190−195.

(7) Takahashi, S.; Wang, J.; Rousseau, D. L.; Ishikawa, K.; Yoshida, T.; Takeuchi, N.; Ikeda-Saito, M. *Biochemistry* **1994**, *33*, 5531−5538.

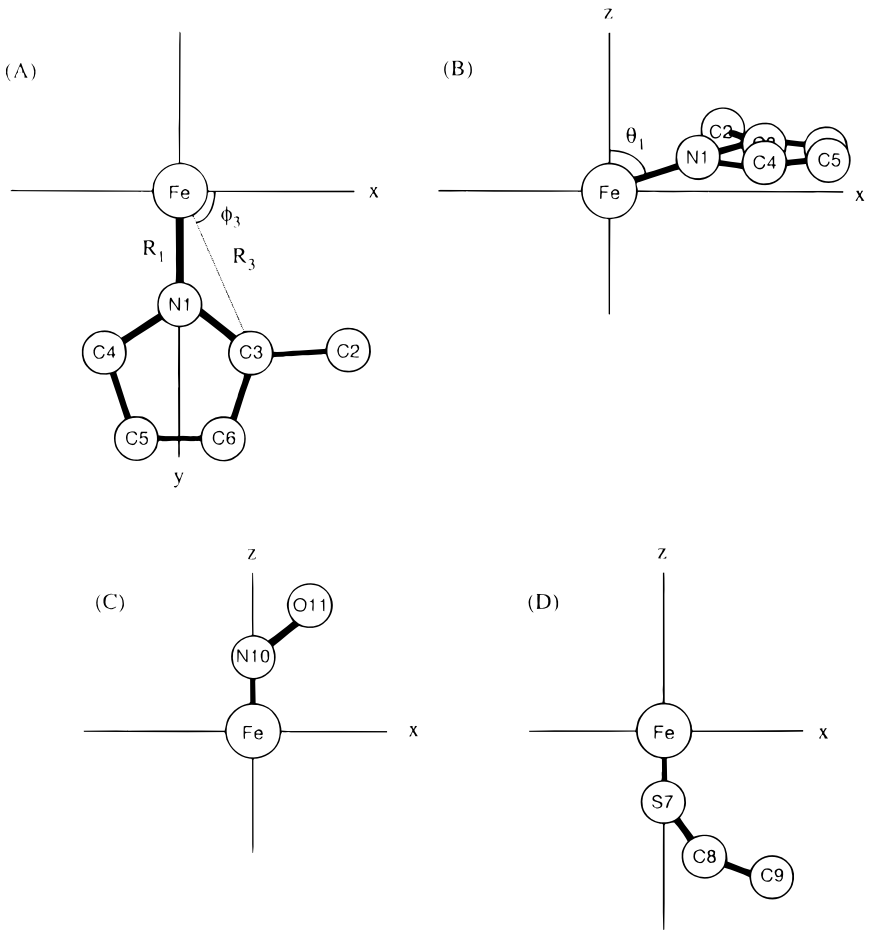

Figure 1. One-fourth of a porphyrin ring (defined as unit 1) which is seen from the direction parallel to (A) *z*- and (B) *y*-axis. The terminology of bond distances and angles and numbering of atoms used are also shown. Atomic positions are described by either by spherical polar (r, θ, ϕ) or Cartesian (x, y, z) coordinates. (C) Cysteine group (S_γ, C_β, and C_α atoms) and (D) sixth ligand (in this case, NO molecule) used for constrained and restrained refinement. Numbering of each atom is also shown.

atoms which are same distance away from the iron atom would have the same value. Refined bond distances (R_n), Debye-Waller terms (α_n), and polar angles (ϕ_n) used in the constrained refinement are compiled in Table 1, together with the *R*-factor of refinement (R_{total}), number of parameters (p), number of independent data points (N_i), minimized sum of squares of residuals (Φ), and fitting index (ϵ_v^2). Definition of these values are the same as Binsted et al.[5] Restrained refinement was carried out starting from the result of the constrained refinement. We minimized the following sum of squares of residuals

$$\Phi = w_{\text{exafs}}\Phi_{\text{exafs}} + w_{\text{distances}}\Phi_{\text{distances}} \quad (1)$$

where w_{exafs} and $w_{\text{distances}}$ are the weighting factors used to define the relative significance of these contributions. Φ_{exafs} is given by

$$\Phi_{\text{exafs}} = \sum (1/\sigma_i^2)(\chi^{\text{exptl}}(k_i) - \chi^{\text{theor}}(k_i))^2 \quad (2)$$

where $\chi^{\text{exptl}}(k)$ and $\chi^{\text{theor}}(k)$ are the experimental and theoretical EXAFS. We normally take σ to be defined by

$$1/\sigma_i = k_i^n / \sum k_j^n |\chi_j^{\text{exptl}}(k_j)| \quad (3)$$

where n is selected so that $k^n\chi^{\text{exptl}}(k)$ has an approximately constant amplitude over the data range used. $\Phi_{\text{distances}}$ is obtained by comparison of refined distances with idealized distances, and given by

$$\Phi_{\text{distances}} = \sum (1/\sigma_i^2)((r_i^{\text{ref}} - r_i^{\text{ideal}})/r_i^{\text{ideal}})^2 \quad (4)$$

with

$$1/\sigma_i = (1/\sigma_i^{\text{dist}})/(\sum 1/\sigma_j^{\text{dist}}) \quad (5)$$

Here, r^{ref} refers to refined distances and r^{ideal} refers to idealized distances. The sum of $w_{\text{exafs}} + w_{\text{distances}}$ must equal 1. In our restrained refinement, we fixed both w_{exafs} and $w_{\text{distances}}$ as 0.5. The values of σ in eqs 4 and 5 for the restrained refinement can be derived from the standard deviation of crystallographic distances for small molecules or by other means, including trial and error. Here, we have assumed that bonded distances have $1/\sigma$ equal to 5 and nonbonded distances have a $1/\sigma$ of 2. Bond distances (R_n), Debye−Waller terms (α_n), and polar angles (ϕ_n) refined by the restrained refinement are also compiled in Table 1. The practical limit for resolving bind distances with a k range of 3−13 Å^{-1} is about 0.05 Å.[5c]

Results

IR Spectra. The ferric NO complexes of both P450nor and P450cam are stable enough for several spectroscopic measurements employed here. Their optical absorption spectra hardly changed over several hours under anaerobic conditions, indicating no autoreduction to its ferrous NO forms and no denaturation of the protein. We measured the IR spectra of the ferric NO-bound form to P450 nor (P450nor(Fe^{3+}NO)) and of P450 cam (P450cam(Fe^{3+}NO)) to examine the frequencies of the iron-bound NO stretching mode. In Figure 2 are illustrated the region of the ^{14}N−O stretching mode for P450nor(Fe^{3+}NO) and P450cam(Fe^{3+}NO) and the ^{14}NO−^{15}NO difference spectrum for P450nor(Fe^{3+}NO). For P450nor(Fe^{3+}NO), the NO stretching (ν(N−O)) was observed at 1851 and 1820 cm^{-1} for the ^{14}NO and ^{15}NO derivatives, respectively (Figure 2B,C). On the other hand, the frequency for the iron-bound NO in P450cam(Fe^{3+}-NO) was located at 1806 cm^{-1} (Figure 2A), which moved to 1775 cm^{-1} upon replacement with ^{15}NO (data not shown). The

Table 1. Parameters Used in the Restrained Refinement of the EXAFS of Cytochrome P450nor and P450cam in the Ferric-NO and Ferric Forms[a]

	Fe^{3+}		Fe^{3+}-NO	
parameters	P450nor	P450cam	P450nor	P450cam
E_0	**−1.57**	**−1.56**	**7.19**	**6.01**
Z_1	0.00	0.43	0.00	0.00
X_1	1.99	1.99	2.00	2.00
R_1	**1.99**	**2.03**	**2.00**	**2.00**
R_2	**3.42**	**3.44**	**3.40**	**3.42**
R_3	**3.06**	**3.07**	**3.05**	**3.05**
R_4	**3.01**	**3.04**	**3.01**	**3.00**
R_5	**4.28**	**4.29**	**4.24**	**4.26**
R_6	**4.23**	**4.25**	**4.24**	**4.26**
R_7	**2.26**	**2.26**	**2.26**	**2.26**
R_8	**3.65**	**3.63**	**3.19**	**3.12**
R_9	**4.09**	**4.13**	**3.86**	**3.82**
R_{10}	**2.44**		**1.66**	**1.76**
R_{11}			**2.79**	**2.84**
α_1	**0.002**	**0.006**	**0.002**	**0.001**
α_2	**0.010**	**0.010**	**0.010**	**0.002**
$\alpha_{3/4}$	**0.006**	**0.007**	**0.003**	**0.002**
$\alpha_{5/6}$	**0.018**	**0.018**	**0.025**	**0.022**
α_7	**0.005**	**0.005**	**0.020**	**0.027**
α_8	**0.006**	**0.010**	**0.023**	**0.030**
α_9	**0.010**	**0.020**	**0.023**	**0.030**
α_{10}	**0.031**		**0.031**	**0.003**
α_{11}			**0.023**	**0.030**
ϕ_2	**45.0**	**45.0**	**43.7**	**44.2**
ϕ_3	**21.3**	**21.3**	**20.6**	**20.6**
ϕ_4	**338.7**	**338.7**	**339.1**	**339.6**
ϕ_5	**9.1**	**9.1**	**8.9**	**9.1**
ϕ_6	**350.9**	**350.9**	**350.8**	**351.1**
ϕ_8	**0.0**	**0.0**	**16.5**	**14.7**
ϕ_9	**5.5**	**5.4**	**8.8**	**6.9**
ϕ_{11}			**0.0**	**0.7**
R_{exafs}	23.9	26.1	31.2	35.0
$R_{distance}$	0.32	0.36	0.68	1.27
R_{total}	24.2	26.4	31.9	36.3
N_i	36.5	36.8	40.4	39.8
p	26	24	29	29
$10^3\Phi$	0.079	0.104	0.147	0.206
$10^6\epsilon_\nu{}^2$	0.267	0.349	0.56	0.780

[a] E_0 is the edge position relative to the photoelectron wave vector; R_n and α_n refer to the distances (in Å) and Debye−Waller terms (in 2 Å^2) for shell n; Φ, ϵ, N_i, p, R_{exafs}, and $R_{distance}$ are defined in Binsted et al.[5b] ϕ_n is the polar angle for shell n. All refined parameters are shown in bold type.

^{14}NO stretching mode of P450nor(Fe^{3+}NO) is higher by 45 cm^{-1} than that of P450cam(Fe^{3+}NO), indicating that the iron-bound N−O bond is stronger in P450nor(Fe^{3+}NO) than in P450cam-(Fe^{3+}NO).

Resonance Raman Spectra. Traces A and B of Figure 3 are the resonance Raman spectra of the ferric resting form of P450nor (P450nor(Fe^{3+})) and of P450nor(Fe^{3+}NO), respectively, in the high-frequency region. In the spectrum of P450nor(Fe^{3+}), the ν_3 mode is split into two lines at 1485 and 1501 cm^{-1}, and the ν_2 is also split at 1567 and 1584 cm^{-1}. The ν_3 at 1501 cm^{-1} and the ν_2 at 1584 cm^{-1} are assigned to be originated from the heme in a ferric low-spin state, while the ν_3 at 1485 cm^{-1} and the ν_2 at 1567 cm^{-1} are from the heme in a ferric high-spin state.[8,9] The Raman spectral feature we observed is consistent with the high- and low-spin mixing state of P450nor(Fe^{3+}) and in good agreement with the optical absorption spectral feature at room temperature.[1e,2c] On the other hand, the ν_3 and ν_2 stretching modes of the NO complex

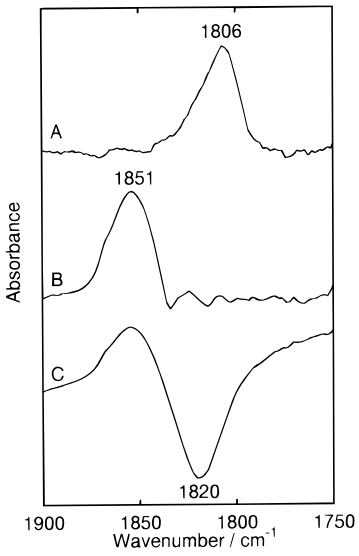

Figure 2. The iron-bound NO stretching region in the IR spectra for (A) P450cam(Fe^{3+}NO) and (B) P450nor(Fe^{3+}NO), and (C) ^{14}NO−^{15}NO difference IR spectrum for P450nor(Fe^{3+}NO). The band width (HWFM) of the ν(N−O) for P450cam was 22 cm^{-1}, whereas that for P450nor was 26 cm^{-1}.

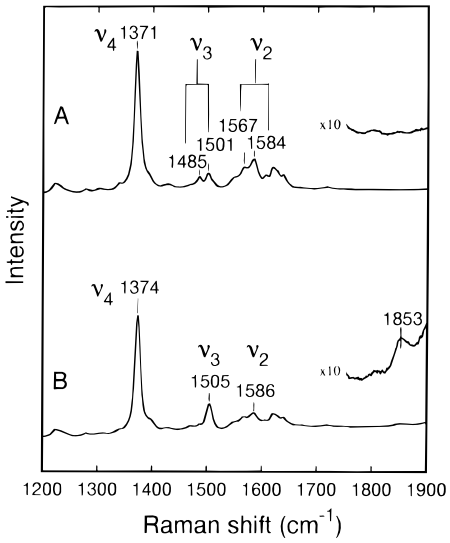

Figure 3. High-frequency region of the resonance Raman spectra of P450nor in (A) the ferric resting and (B) the ferric-NO sates. Inset shows the 10× expansion of the region for the NO stretching mode.

were located at 1505 and 1586 cm^{-1}, respectively, showing a pure ferric low-spin state.[7,8]

In spectral comparison between P450nor(Fe^{3+}) and P450nor(Fe^{3+}NO), we found that a new and weak line appeared at 1853 cm^{-1} upon the NO binding (see Figure 3B). The ^{14}N/^{15}N substitution of the NO ligand caused this line to shift to 1816 cm^{-1}, as shown as traces A, C, and E of Figure 4. From the similarity in its frequency and the ^{14}N/^{15}N substitution effect between the Raman and IR spectra (see Figure2), we assigned this band to the N−O stretching mode (ν(N−O)) in P450nor-(Fe^{3+}NO). In the Raman spectrum of P450cam(Fe^{3+}NO), we also identified the ν(N−O) at 1805 cm^{-1} (data not shown).

In Figure 5 are illustrated the resonance Raman spectra of P450nor(Fe^{3+}NO) in the low-frequency region. The spectral feature in this region (Figure 5A) was similar to that of P450nor-(Fe^{3+}) (data not shown), except for the line at 530 cm^{-1}, which was undetectable in the spectrum of P450nor(Fe^{3+}). Upon substitution of the ^{14}NO ligand with ^{15}NO, this line shifted to 525 cm^{-1} (Figure 5C,E), indicating that the line comes from

(8) Spiro, T. G.; Stong, J. D.; Stein, P. *J. Am. Chem. Soc.* **1979**, *101*, 2648−2655.
(9) (a) Hu, S.; Kincaid, J. R. *J. Am. Chem. Soc.* **1991**, *113*, 2843−2850; (b) *J. Biol. Chem.* **1993**, *168*, 10512−10516.

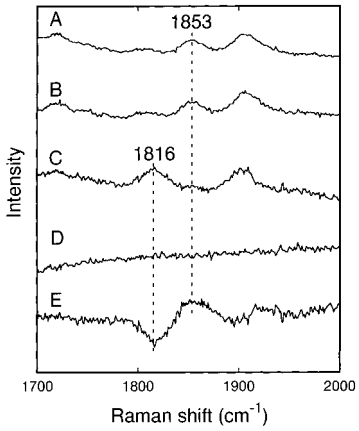

Figure 4. The NO stretching mode in the resonance Raman spectra for P450nor(Fe^{3+}NO) in (A) the ^{14}NO complex in H_2O, (B) the ^{14}NO complex in D_2O, and (C) the ^{15}NO complex in H_2O. D is the difference spectrum of A−B ($H_2O - D_2O$). E is the difference spectrum of A−C ($^{14}NO - {}^{15}NO$). The peak around 1900 cm^{-1} was insensitive to the ^{14}NO/^{15}NO substitution.

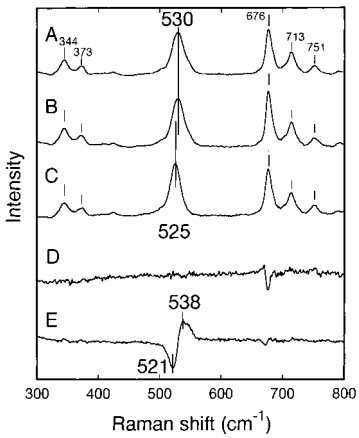

Figure 5. Low-frequency region of the resonance Raman spectra of P450nor(Fe^{3+}NO) in (A) the ^{14}NO complex in H_2O, (B) the ^{14}NO complex in D_2O, and (C) the ^{15}NO complex in H_2O. D is the difference spectrum of A−B ($H_2O - D_2O$). E is the difference spectrum of A−C ($^{14}NO - {}^{15}NO$), where the contributions from the porphyrin modes balance, revealing the isotopic shift. The lines at 344 and 373 cm^{-1} can be assignable to the vibrational mode of the porphyrin skelton. The laser excitation wavelength was 413nm.

the Fe−N−O moiety of P450nor(Fe^{3+}NO). We compared the spectrum of P450nor(Fe^{3+}NO) with that of P450cam(Fe^{3+}NO) reported by Hu and Kincaid,[9] in which the Fe−NO stretching (ν(Fe−NO)) and the Fe−N−O bending frequencies (δ(Fe−N−O)) were located at 522 and 546 cm^{-1}, respectively. They also showed that the ν(Fe−NO) and the δ(Fe−N−O) moved to 520 cm^{-1} ($\Delta = 2$ cm^{-1}) and 533 cm^{-1} ($\Delta = 13$ cm^{-1}), respectively, upon the ^{15}NO substitution. Judging from the isotope shift ($\Delta = 5$ cm^{-1}), we assigned the line observed at 530 cm^{-1} for P450nor(Fe^{3+}NO) to the ν(Fe−NO).

The result demonstrated that the ν(Fe−NO) of P450nor(Fe^{3+}-NO) is located 8 cm^{-1} higher than that of P450cam(Fe^{3+}NO). In addition, it is also noted that the δ(Fe−N−O) is undetectable in the spectrum of P450nor(Fe^{3+}NO), as is the case for the norcamphor-bound and substrate-free forms of P450cam(Fe^{3+}-NO).[9] According to Hu and Kincaid, the absence of the δ-(Fe−N−O) is indicative of binding of NO to the ferric iron along the heme normal, *i.e.*, the linear Fe−N−O configuration.[9,10]

(10) Yu, N.-T.; Kerr, E. A.; Ward, B.; Chang, C. K. *Biochemistry* **1983**, *22,* 4534.

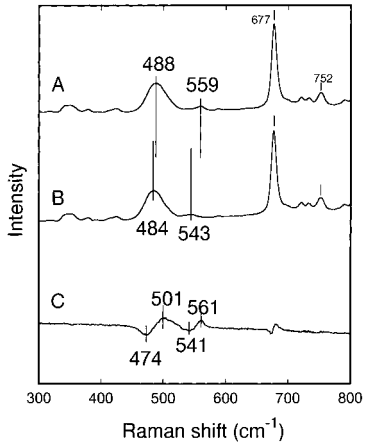

Figure 6. Low-frequency region of the resonance Raman spectra of P450nor(Fe^{2+}CO) in (A) the ^{12}CO complex, (B) the ^{13}CO complex, and (C) the difference spectrum of A − B ($^{12}CO - {}^{13}CO$), where the contributions from the porphyrin modes balance, revealing the isotopic shift. The laser excitation wavelength was 441nm.

To examine an interaction of the Fe-bound NO with its surroundings, we measured the resonance Raman spectra in D_2O for the high- and low-frequency regions, as illustrated in Figures 4B and 5B, respectively, and compared them with the corresponding spectra measured in H_2O (Figures 4A and 5A). However, no differences were observed in either the high- or low-frequency regions (see Figures 4D and 5D), especially in the ν(N−O) and the ν(Fe−NO), showing no strong hydrogen-bonding interaction of the iron-bound NO with its surroundings.

We also measured the resonance Raman spectrum of the ferrous CO-bound form of P450nor (P450nor(Fe^{2+}CO)) to detect the ν(Fe−CO) and the δ(Fe−C−O). The ν(Fe−CO) and δ-(Fe−C−O) of P450nor(Fe^{2+}CO) were observed at 488 and 559 cm^{-1}, respectively, and were shifted to 484 and 543 cm^{-1} upon substitution of ^{12}CO with ^{13}CO, as illustrated in Figure 6. On the other hand, the ν(Fe−CO) and the δ(Fe−C−O) of the ferrous CO-bound form of P450cam (P450cam(Fe^{2+}CO)) were reported to be observed at 484 and 558 cm^{-1}, respectively.[11,12] It was found, therefore, that the Fe−ligand stretching frequency for the ferrous-CO complex locates 4 cm^{-1} higher in P450nor than in P450cam, as is the case for the ferric-NO complex.

In Figure 7A, the frequencies of ν(Fe−NO) and ν(N−O) modes for P450nor(Fe^{3+}NO) obtained in the present study are compared with those obtained for other S^--coordinated hemoproteins. The corresponding plot for P450nor(Fe^{2+}CO) and other proteins is presented in Figure 7B. For the Fe^{3+}NO compounds, we measured the ν(N−O) in the IR spectra of P450cam(Fe^{3+}NO) in the presence and absence of some substrates [substrate-free (1806 cm^{-1}), norcamphor (1818 cm^{-1}), and adamantanone (1818 cm^{-1})] and chloroperoxidase(Fe^{3+}-NO) (1868 cm^{-1}) (Makino, R. private communication) and then plotted them against the ν(Fe−NO) reported by Hu and Kincaid.[9] In both plots of ν(Fe−NO) vs ν(N−O) and ν(Fe−CO) vs ν(C−O), the points for P450nor locate well within the line formed by the other proteins, suggesting that the vibrational characters of the Fe^{3+}−N−O and the Fe^{2+}−C−O units are not severely deviated from the other S^--coordinated hemoproteins. It is noteworthy that the correlation shows an opposite trend between the Fe^{3+}NO and the Fe^{2+}CO complexes; the ν(Fe−NO) increases with increasing the ν(N−O), while the ν(Fe−CO) behaves inversely to the ν(C−O). The result is

(11) Wells, A. V.; Li, P.; Champion, P. M.; Martinis, S. A.; Sligar, S. G. *Biochemistry* **1992**, *31,* 4384−4393.

(12) Uno, T.; Nishimura, Y.; Makino, R.; Iizuka, T.; Ishimura, Y.; Tsuboi, M. *J. Biol. Chem.* **1985**, *260,* 2023−2026.

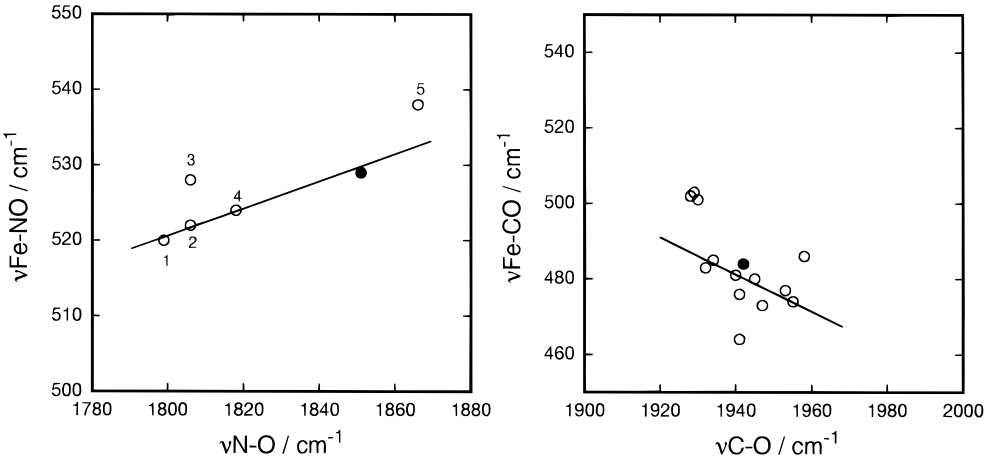

Figure 7. Plots of observed (A) ν(Fe−NO) vs ν(N−O) and (B) ν(Fe−CO) vs ν(C−O) frequencies in the $Fe^{3+}NO$ and the $Fe^{2+}CO$ complexes, respectively, for the S^--coordinated hemoproteins and their model compounds. In both plots, the closed circles show the data of P450nor. In A, the numbers correspond to the data: (1) P450cam + adamantanone, (2) P450cam + camphor, (3) substrate-free P450cam, (4) P450cam + norcamphor, (5) chloroperoxidase.

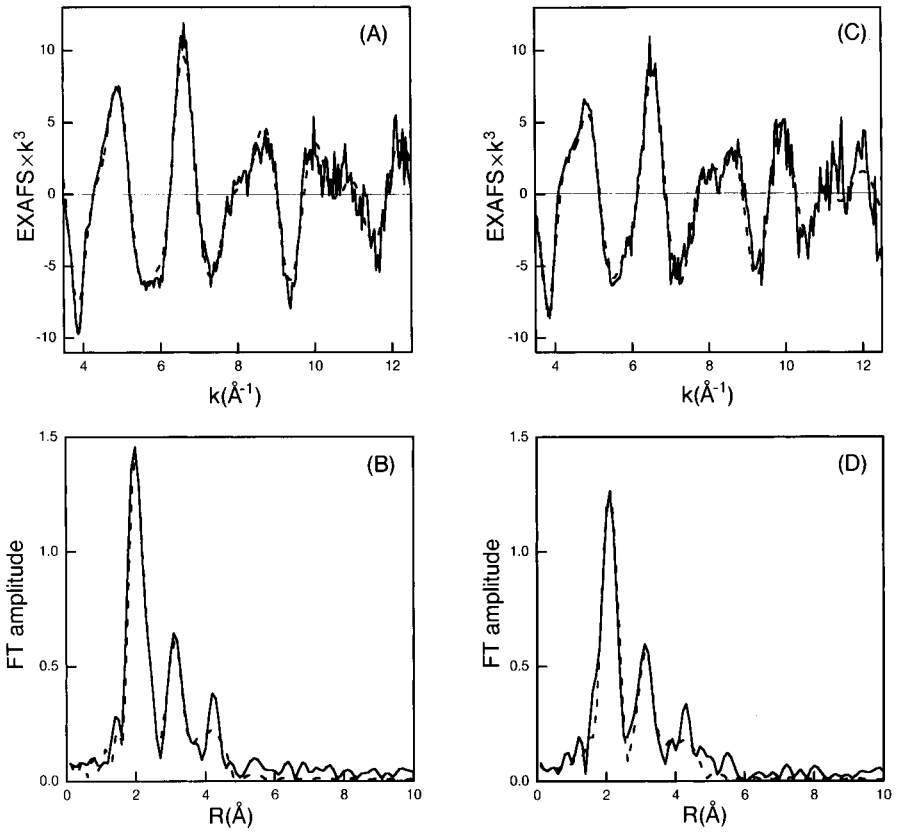

Figure 8. The EXAFS spectra (weighted by k_3) for (A) P450nor(Fe^{3+}) and (C) P450cam(Fe^{3+}). B and D are the Fourier transforms of A and C, respectively. The raw data (solid line) and its curve-fitting result (dotted line) are shown.

suggestive of the difference in the bond character of the iron and the ligand between these two complexes, which will be discussed later.

EXAFS. In Figures 8 and 9, we compared the Fe K-edge EXAFS and their Fourier transforms between P450nor and P450cam for the ferric resting state (Figure 8) and for the ferric-NO complex (Figure 9). The fitting of all the data by EXCURV92 was sufficiently good enough to give the distance of the innershell of the iron coordination sphere (Fe−N_{Por}, Fe−S_{Cys}, Fe−O_{H2O}, Fe−N_{NO}, and Fe−Ct), where the d(Fe−Ct) represents the distance of the iron from the center of the pyrrole plane. These data were compiled and compared between the two enzymes in Table 2. The index of goodness of fit, ϵ_ν^2, was sufficiently small as shown in Table 1.[5b] When the fitting was started from the different initial values, the same result was obtained.

In the ferric resting enzyme of P450cam, our data for P450cam(Fe^{3+}) are identical to those reported by Hahn et al.,[13] which showed the five-coordinated heme iron. In contrast, the first Fourier peak of P450nor(Fe^{3+}) (Figure 8B) is significantly higher in its intensity than that of P450cam(Fe^{3+}), which suggested a coordination of the sixth ligand to the heme iron of P450nor(Fe^{3+}). When we assumed the coordination of a water molecule as the sixth ligand in P450nor(Fe^{3+}), we

(13) Hahn, J. E.; Hodgson, K. O.; Andersson, L. A.; Dawson, J. H. *J. Biol. Chem.* **1982**, *257*, 10934−10941.

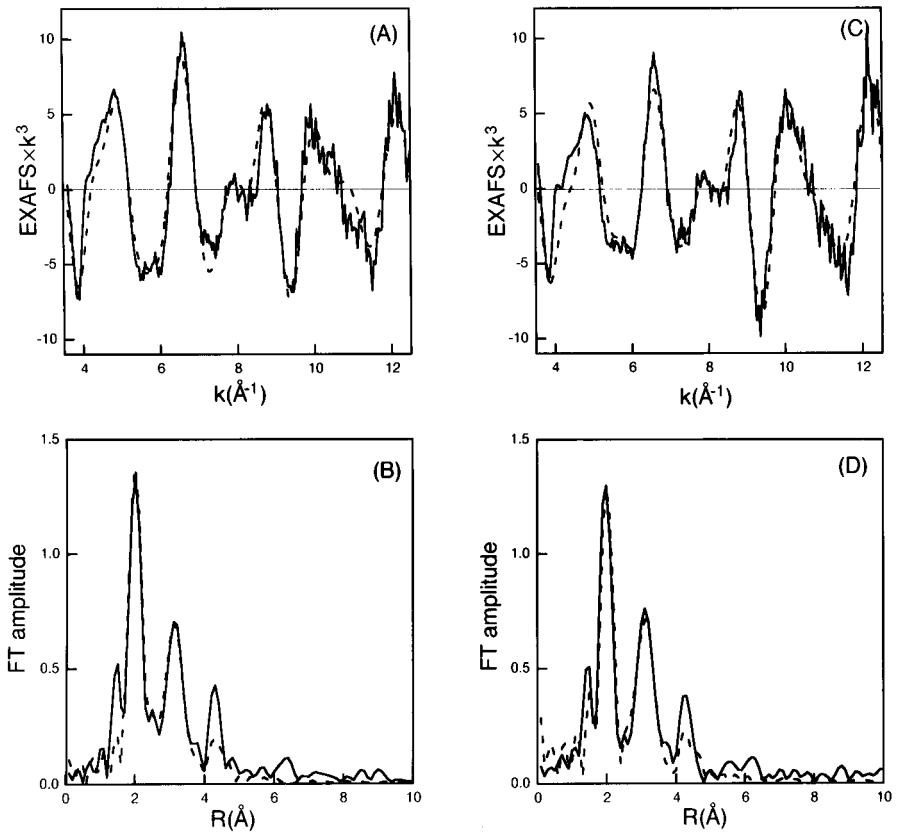

Figure 9. The EXAFS spectra (weighted by k_3) for (A) P450nor(Fe^{3+}NO) and (C) P450cam(Fe^{3+}NO). B and D are the Fourier transforms of A and C, respectively. The raw data (solid line) and its curve-fitting result (dotted line) are shown.

Table 2. Comparison of Iron−Ligand Atom Distances for Cytochrome P450nor and P450cam in the Ferric, Ferric-NO, Ferrous, and Ferrous-CO Forms Elucidated by EXAFS[a]

complexes		Fe−N_{Por} (Å)	Fe−S_{Cys} (Å)	Fe-O_{H2O} (Å)	Fe−N_{NO} (Å)	Fe−Ct (Å)
Fe^{3+}	P450nor	1.99	2.26	2.44		0.00
	P450cam	2.03	2.26			0.43
Fe^{3+}-NO	P450nor	2.00	2.26		1.66	0.00
	P450cam	2.00	2.26		1.76	0.03

[a] The parameters used to simulate the K-edge EXAFS are basically the same as those in Table 1 of Binsted et al.[5b] Distances and Debye−Waller terms of the fifth cysteinyl ligand and a sixth ligand molecule (NO or H_2O), if any, are also included. Debye−Waller terms belonging to the same shell of atoms were paired together during refinement. The least-squares fitting errors were in the range of ±0.003−0.007 Å for distances and ±0.0009−0.0025 Å^2 for the Debye−Waller terms. Errors given in the text are conservative estimates for absolute values of distance. Error given in the text are conservative estimations derived from comparison of bond distances of model compounds between the authentic distances determined from crystallographic and calculated distances with EXCURV92. The accuracy for determining a relative change in coordination distance is comparable to the fitting error. Then, the iron−ligand bond distances were determined in the first coordination shell to an accuracy of ±0.02 Å.

obtained better fitting result, compared with that using five-coordinated heme iron. As mentioned above, the ferric resting enzyme at room temperature is in a mixed state of high-spin (H_2O-free) and low-spin (H_2O-bound) forms. However, in a frozen state at 77 K, the iron is predominantly in a ferric low-spin state, most probably due to the water coordination, which was studied with the EPR and optical absorption spectral measurements.[2d] Thus, the EXAFS result is consistent with this structural characteristic. Resulting from the sixth water coordination, the iron is pulled up into the heme plane (d(Fe−Ct) = 0.0 Å; in-plane coordination), in sharp contrast to the out-of-plane configuration of P450cam (d(Fe−Ct) = 0.44 Å). The magnitude of the iron displacement in P450cam is in good agreement with the value reported from the crystallographic data.[14]

In the ferric-NO complexes, it was found that the d(Fe−N_{Por}) and d(Fe−S_{Cys}) are indistinguishable between the two enzymes and that the iron of the both enzymes is located in the heme plane, most probably due to the strong NO binding. On the other hand, the d(Fe−N_{NO}) in P450nor (1.66 Å) is shorter by 0.1 Å than that in P450cam (1.76 Å). Both enzymes employed for the EXAFS measurement evidently gave the optical absorption spectra characteristic to the ferric-NO complex of the P450, and the error estimation of the EXAFS analysis is indicative of uncertainty of ±0.02 Å (see footnote of Table 1), showing that d(Fe−N_{NO}) values from our EXAFS measurements and analyses are reliable with the uncertainty. The Fe−N−O angles of the two enzymes are calculated to be nearly 180° as shown in Table 1 (see ϕ_{11}), but this angle did not seriously affect the fitting results of the bond distances in the range of 160−180°.

Recently, we reported the d(Fe−C_{CO}) in P450nor(Fe^{2+}CO) as 1.74 Å, which is shorter than that (1.76 Å) in P450cam-(Fe^{2+}CO).[15] When this is combined with the present Raman data (Figure 6), we can suggest that the Fe−CO bond is considerably stronger in P450nor than in P450cam, as for the ferric NO complex. The difference (0.02 Å) in the d(Fe−C_{CO}) appears to be larger than that expected from the difference (4 cm^{-1}) in the ν(Fe−CO) between the two proteins. According to the discussion by Ray et al.,[16] a bond compression of 0.01 Å corresponds to a ν(Fe−CO) elevation of 6 cm^{-1}. Since the observed difference in d(Fe−C_{CO}) is within the uncertainty of

(14) Poulos, T. L.; Finzel, B. C.; Howard, A. J. *J. Mol. Biol.* **1987**, *195*, 687−700.
(15) Shiro, Y.; Tsukamoto, K.; Obayashi, E.; Adachi, S.; Iizuka, T.; Nomura, M.; Shoun, H. *J. Phys. IV* In press.
(16) Ray, G. B.; Li, X.-Y.; Ibers, J. A.; Sessler, J. L.; Spiro, T. G. *J. Am. Chem. Soc.* **1994**, *116*, 162−176.

our EXAFS analysis (<0.02 Å), we interpret that the apparent discrepancy between the EXAFS and Raman data may be artificial. On the contrary, the difference in the d(Fe−N_{NO}) between P450nor and P450cam (0.1 Å) is above the experimental uncertainty and seems to be much larger than the observed difference (8 cm^{-1}) in the ν(Fe−NO). We will discuss this apparent discrepancy in the data obtained by different spectroscopies in the next section.

Discussion

The present results obtained from the X-ray absorption and vibrational spectroscopies revealed significant differences in the NO coordination to the ferric heme iron between P450nor and P450cam, which were manifested by the differences in d(Fe−N_{NO}), ν(Fe−NO), and ν(N−O). Since the ferric-NO complex of P450nor is a primary intermediate of the NO reduction cycle, the difference in the NO binding possibly correlates to the difference in the catalytic property between P450nor and P450cam.

***Trans* Effect.** Before discussing the NO binding to the P450s, we refer the NO coordination in the Fe^{3+}NO porphyrin model compounds, *i.e.*, [Fe(OEP)(NO)]ClO_4 and [Fe(TPP)(NO)-(H_2O)]ClO_4 (where OEP = octaethylporphyrin and TPP = tetraphenylporphyrin), which were studied by Scheidt et al.[17a] with X-ray crystallography. In the five-coordinated [Fe(OEP)-(NO)]ClO_4, the NO ligand linearly binds to the iron with the d(Fe−N_{NO}) of 1.64 Å, and the iron is displaced toward the NO ligand due to its strong binding, forming an out-of-plane configuration (d(Fe−Ct) = 0.32 Å). In [Fe(TPP)(NO)(H_2O)]-ClO_4, the H_2O coordination at the opposite site of the bound NO pulls the iron into the heme plane (d(Fe−Ct) = 0.0 Å; the in-plane configuration), but does not affect the d(Fe−N_{NO}) (1.65 Å). Scheidt and his co-workers also reported the iron coordination geometry of the Fe^{2+}NO model compounds, *e.g.*, d(Fe−N_{NO}) = 1.74 Å and d(Fe−Ct) = 0.04 Å for Fe(TPP)NO(1-methylimidazole).[17b]

As seen in Table 2, the d(Fe−N_{NO}) of P450cam(Fe^{3+}NO) is similar to that of the Fe^{2+}NO model compound rather than those of the Fe^{3+}NO model compounds. This can be reasonably explained in terms of the ligation effect of the strong electron donor (S^-) to the ferric heme iron as a fifth axial ligand,[14] although the structure of the S^- adduct of the Fe^{3+}NO porphyrin model compound is not yet available. Due to the effect of the electron donation from the S^- through a $3p_y$−$3d_\pi$ interaction (π bonding) as well as a $3p_z$−$3d_{z^2}$ interaction (σ bonding), it has been generally considered that its ferric heme iron exhibits the Fe^{2+} character rather than Fe^{3+} character toward the ligand binding at the sixth site in P450s (*trans* effect).

Comparison of the d(Fe−S_{Cys}) between P450nor(Fe^{3+}NO) and P450cam(Fe^{3+}NO) obtained from our EXAFS analysis (Table 2) shows that the Fe−S_{Cys} bond of P450nor(Fe^{3+}NO) is the same in its strength as that of P450cam(Fe^{3+}NO). However, the d(Fe−N_{NO}) of P450nor(Fe^{3+}NO) is different from that of P450cam(Fe^{3+}NO). The distance is comparable to those of the Fe^{3+}NO model compounds rather than that of the Fe^{2+}NO model compound. We can rule out the difference in the *trans* effect on the Fe−NO bond derived from the difference in the Fe−S^- bond and can suggest that other factors, probably from surroundings of the NO ligand, is different between P450nor and P450cam, resulting in the different NO coordination.

Fe^{3+}NO Electronic Configuration. Here, we refer the relationship of the electronic configuration of the NO derivatives to their N−O stretching mode, which has been already evaluated.[18] The free and neutral NO molecule has a single electron in its 2pπ* orbital, giving a N−O stretching frequency at 1840 cm^{-1}. The removal of a 2pπ* electron forms NO^+. The resultant NO^+ gives its stretching mode at 2300 cm^{-1}, showing an increase in bond order in going from NO to NO^+. Conversely, the addition of an electron forms NO^- and shifts its stretching mode to 1290 cm^{-1}, *i.e.*, a decrease in the bond order. When the NO molecule is bound to the metal, *e.g.*, the iron in our case, the position of the ν(N−O) is a result of combination of σ and π bonding and back-bonding characters between the iron and the NO orbitals. For example, the ν(N−O) of Mb(Fe^{3+}NO) was observed at 1921 cm^{-1} (data not shown), where the iron-bound NO exhibits NO^+ characteristics. When this is combined with the Raman observation by Benko and Yu,[19] where the ν(Fe−NO) of Mb(Fe^{3+}NO) was observed at 594 cm^{-1}, the vibrational spectral results are indicative of dominance in the donation of the NO 2pπ* electron to the Fe^{3+} orbital through the π bond. This electronic configuration in the Fe^{3+}−NO bond is consistent with the property of Mb(Fe^{3+}-NO), which is readily autoreduced to its ferrous form.

For the NO ligand coordinated to the heme iron of P450s, the S^- ligand at the fifth position donates the π electron to the NO 2pπ antibonding (2pπ*) orbital through the iron 3dπ orbital (π back-donation). This electronic configuration bestows on the NO ligand an anionic character. This is the case for P450cam, in which the ν(N−O) appears at a lower frequency (1806 cm^{-1}) than that of free NO. However, our IR results (see Figure 2) showed that the coordinated NO molecule in P450nor(Fe^{3+}NO) exhibits almost identical ν(N−O) as that of free NO, which indicates a neutral character of the NO ligand. Since the Fe−S^- bond strengths (*trans* effect) are the same for both enzymes, we can consider that the donation of the NO 2pπ* electron to the iron 3dπ orbital (π donation) as well as the σ donation from the NO 2pσ to the iron 3dσ orbitals are more facilitated in P450nor(Fe^{3+}NO), compared with that of P450cam(Fe^{3+}NO), possibly by some steric and/or electrostatic effects on the bound NO from its surroundings. This can account for both of the Fe−NO and the N−O bonds in P450nor-(Fe^{3+}NO) being stronger than the corresponding ones in P450cam(Fe^{3+}NO).

Participation of the NO 2pπ* electron into the bond formation results in the "normal" correlation in the plot of ν(Fe−NO) vs ν(N−O) for some S^--coordinated hemoproteins (Figure 7A); as the ν(Fe−NO) increases, the ν(N−O) also increases. The bond character is contrasted with that in a ferrous CO complex; due to the absence of the CO 2pπ* electron, the Fe^{2+}−CO bond is governed by both the σ donation from the CO ligand to the iron and the π back-donation from the iron to the CO ligand, giving the inverse correlation between the ν(Fe−CO) and ν-(C−O) (see Figure 7B).

Our IR[20] and Raman (Figure 6) measurements showed that the ν(C−O) and the ν(Fe−CO) are observed at 1940 and 488 cm^{-1}, respectively, for P450nor, which are comparable to those for P450cam (1940, 484 cm^{-1}).[2a] The observations revealed the Fe−CO bond to be stronger in P450nor than in P450cam and that the σ donation is enhanced more in P450nor than in P450cam. The combined results for the ferric-NO and the ferrous-CO bindings suggest that there are some specific effects

(17) (a) Scheidt, W. R.; Lee, Y. J.; Hatano, K. *J. Am. Chem. Soc.* **1984**, *106*, 3191−3198. (b) Scheidt, W. R.; Piciulo, P. L. *J. Am. Chem. Soc.* **1976**, *98*, 1913−1919.

(18) (a) Stamler, J. S.; Singel, D. J.; Loscalzo, J. *Science* **1992**, *258*, 1898−1902. (b) Tsai, A. *FEBS Lett.* **1994**, *341*, 141−145.

(19) Benko, B.; Yu, N.-T. *Proc. Natl. Acad. Sci. U.S.A.* **1983**, *80*, 7042−7046.

(20) Jung, C.; Hoa, G. H. B.; Schröder, K.-L.; Simon, M.; Doucet, J. P. *Biochemistry* **1992**, *31*, 12855−12862.

around the ligand binding site of P450nor to facilitate both the σ and the π donation from the external ligand to the iron.

Steric Effect. We measured the NO association rate constants for P450nor(Fe^{3+}) and P450cam(Fe^{3+}) at 20 °C using the flash photolysis technique,[2c] and obtained 1.9×10^7 M^{-1} s^{-1} for P450nor(Fe^{3+}) and 7.5×10^5 M^{-1} s^{-1} for P450cam-(Fe^{3+}) (Obayashi, E.; Shiro, Y., unpublished results). It was found that the NO binding to P450nor(Fe^{3+}) is 25 times faster than that to P450cam(Fe^{3+}). This was also the case for the CO binding to the ferrous enzymes as we reported previously,[2a] suggesting that the heme pocket of P450nor is sterically less hindered toward the external ligand than that of P450cam. In other words, the heme pocket of P450nor is larger in size or less crowded than that of P450cam.

Recently, Hu and Kincaid reported that the Fe−NO bond strength in P450cam(Fe^{3+}NO) is markedly influenced by a steric interaction with its surrounding, on the basis of its resonance Raman spectra in the presence and absence of some organic substrates.[9] They found that the ν(Fe−NO) as well as its isotope shift ($\Delta = \nu$(Fe−^{14}NO) − ν(Fe−^{15}NO)) shifted consistently as substrate size increased: 528 cm^{-1} (Δ = 4 cm^{-1}) for the substrate-free enzyme, 524 cm^{-1} ($\Delta = 3$ cm^{-1}) for norcamphor-bound enzyme, 522 cm^{-1} ($\Delta = 2$ cm^{-1}) for the camphor-bound enzyme, and 520 cm^{-1} for the adamantanone-bound enzyme. In this order, the Fe−NO bond becomes weaker. In addition, it is also of interest that the δ(Fe−N−O) is enhanced in the Raman spectra of the camphor- and the adamantanone-bound enzymes, while it was undetectable in those of the substrate-free and the norcamphor-bound enzymes. On the basis of these results and theoretical calculations, they suggested that, upon bending of the Fe−N−O geometry exposed by the bound substrate, the Fe−NO bond is weakened.

Accordingly, we can expect that, due to less steric hindrance in the heme pocket, the Fe−N−O is linear or less bent in P450nor(Fe^{3+}NO), relative to P450cam(Fe^{3+}NO), resulting in the ν(Fe−NO) mode being in a higher frequency region, the larger isotope shift (Δ = 5 cm^{-1}) for the ν(Fe−NO), and the disappearance of the δ(Fe−N−O) mode in its Raman spectrum.[9,10] This also agrees with our EXAFS observation that the Fe−NO bond in P450nor is shorter than that in P450cam.

The remaining problem is that the difference in the d(Fe−N_{NO}) by 0.1 Å seems much larger than that expected from the difference in the ν(Fe−NO) frequency (8 cm^{-1}); the expectation is based on the analyses for ferrous-CO complexes.[16] We do not have a quantitative explanation for this apparent discrepancy, because there have not yet been detailed characterization and analyses for the Fe^{3+}−NO bonds in hemoproteins so far. However, we believe that the bent Fe−NO conformation for P450cam causes the kinematic mixing of the Fe−NO stretching and the Fe−N−O bending modes, which will make it difficult to directly compare ν(Fe−NO) and d(Fe−N_{NO}). For example, the vibrational analyses of the Fe−NO unit of P450cam[9] have shown that the force constants for the Fe−NO stretching bond for the ferric state ($K = 3.15$ mdyn/A) is considerably different from that of the ferrous state (2.44 mdyn/A). The force constant of the bond can be directly comparable to the bond length. However, in spite of the big difference in the force constant, their ν(Fe−NO) appears within 30 cm^{-1}. In addition, while the ferric protein has higher force constant, it shows lower ν(Fe−NO) than that of the ferrous form. These are possibly caused by the difference in the Fe−N−O configuration, *i.e.*, linear for the ferric and bent for the ferrous states, and/or the difference in interaction of the iron-bound NO with its surroundings due to the difference in the oxidation state. These discussions would suggest that the ν(Fe−NO) and the d(Fe−N_{NO}) are varied in some extent, depending on the surrounding condition. Therefore, we interpret that the discrepancies obtained from the EXAFS analysis and the resonance Raman data might indicate the different conformations and/or the different interaction of the Fe−NO unit with its surrounding between P450nor and P450cam.

Electrostatic Interaction. EXAFS results of the ferric resting enzymes (Figure 8 and Table 2) clearly demonstrated water coordination at the heme sixth site of P450nor(Fe^{3+}) and vacancy at this site in P450cam(Fe^{3+}). This suggests that the chemical environment in the heme pocket is considerably different, and such differences might substantially influence the ligand binding properties and structures between these two enzymes. Indeed, comparison of the hydropacy profile suggested that the amino acid side chains constructing the heme pocket of P450nor are more hydrophobic than those in P450cam.[1e] In addition, more negative redox potential in the Fe^{3+}/Fe^{2+} couple for P450nor (−307 mV) than that for P450cam (−140 mV)[2d] implies that the charge balance in the heme pocket is either more negative or less positive in P450nor than in P450cam.

In this context, it is interesting to note that the O_2 complex of P450nor is so unstable that it cannot be detected even at −16 °C due to its rapid autoxidation to the ferric form, in sharp contrast to the relatively stable O_2 complex of P450cam.[21] Since the stability of the O_2 complex of hemoproteins is markedly affected by the electrostatic interaction of the iron-bound O_2 with its surroundings including hydrogen bonding and so on,[22] the extreme instability of the O_2 complex of P450nor, compared with that of P450cam, is indicative of a difference in the electrostatic interaction of the iron-bound ligand with its surroundings between these two enzymes. Therefore, it seems possible that this difference is responsible for the difference in the NO coordination between P450nor(Fe^{3+}NO) and P450cam-(Fe^{3+}NO).

Most recently, Shimizu and his co-workers reported the mutation work of P450 1A2,[23] in which they showed that substitution of Glu318 with Ala enhances the autoreduction rate of the ferric-NO complex to its ferrous form. On the basis of this observation, they suggested that the Fe^{3+}−NO state in P450 is stabilized through the hydrogen-bonding interaction with carboxylic acid of Glu, but removal of this interaction by the mutation facilitates the electron donation from the NO ligand to the ferric iron, resulting in the autoreduction of the ferric-NO complex, as is the case for Mb(Fe^{3+}NO) (*vide supra*). Here, it is noteworthy that the Glu318 of P450 1A2 locates adjacent to the conserved Thr at the distal side and corresponds to Ala242 in P450nor, which does not have hydrogen-bonding ability. Indeed, we evaluated the no hydrogen-bonding interaction of the iron-bound NO in P450nor(Fe^{3+}NO) from the H_2O/D_2O effect on the resonance Raman spectra (see Figures 4 and 5). Thus, we can expect that the absence of the hydrogen-bonding interaction in the iron-bound NO might be attributable to the relatively strong Fe^{3+}−NO bond in P450nor.

The present X-ray absorption and vibrational spectral experiments show possibilities of steric and electrostatic interactions

(21) (a) Ishimura, Y.; Ullrich, V.; Peterson, J. A. *Biochem. Biophys. Res. Commun.* **1971**, *42*, 140−146. (b) Bangcharoenpaurpong, O.; Rizos, A. K.; Champion, P. M.; Jollie, D.; Sligar, S. G. *J. Biol. Chem.* **1986**, *261*, 8089−8092. (c) Hu, S.; Schneider, A. J.; Kincaid, J. R. *J. Am. Chem. Soc.* **1991**, *113*, 4815−4822.

(22) (a) Brantley, R. E., Jr.; Smerdon, S. J.; Wilkinson, A. J.; Singleton, E. W.; Olson, J. S. *J. Biol. Chem.* **1993**, *268*, 6995−7010. (b) Shiro, Y.; Iwata, T.; Makino, R.; Fujii, M.; Isogai, Y.; Iizuka, T. *Ibid*. **1993**, *268*, 19983−19990.

(23) Nakano, R.; Sato, H.; Watanabe, A.; Ito, O.; Shimizu, T. *J. Biol. Chem.* **1996**, *15*, 8570−8574.

influencing the $Fe^{3+}-NO$ bond. At the present stage, we cannot exactly determine which factor is more important in controlling the NO binding strength to the ferric iron in P450s, but most probably, it is a combination of both interactions of the iron-bound NO with its surroundings.

Relevance to NO Reduction Activity. In the catalytic reaction of the NO reduction by P450nor, there are two characteristic properties we should note. First, the electrons used for the NO reduction are transferred from NADH to the heme without any help from other redox proteins such as flavo- and iron−sulfur proteins, *i.e.*, direct electron transfer from NADH to the heme.[1e] This is sharply contrast with the monooxygenation reaction by usual P450s, where the flavo- and iron−sulfur proteins modulate the two-electron-transfer step to the one-electron-transfer step from NAD(P)H to the heme.[3] It is also noted that NADH specifically acts as an electron donor in the *F. oxysporum* NO reduction system but NADPH does not. On the other hand, another fungal NOR from *Cylindrocarpon tonkinense* requires NADPH as the electron donor.[24] Keeping in mind these experimental facts, we speculate that the NADH binding site may be present near the heme site of P450nor and that direct two-electron-transfer, thus, can be allowed from NADH to the heme to form the characteristic intermediate proposed in our hypothetical reaction mechanism.[2c]

The second characteristic property is that P450nor($Fe^{3+}NO$) can be reduced with NADH, but P450nor(Fe^{3+}) cannot.[1e] We have two possible explanations for this observation. (1) NADH can bind to the enzyme in the ferric NO form, but not in the ferric resting from. (2) NADH can bind to both forms, but the electron transfer can occur only in the ferric NO complex. We have not yet found any direct evidence as to which possibility is preferable. However, the present spectroscopic results of P450nor($Fe^{3+}NO$) showed that electron density on the ferric iron-bound NO is relatively low due to the strong NO coordination and that eventually the NO in P450nor becomes neutral. Therefore, we can only suggest that the iron-bound NO in P450nor exhibits an electronic configuration which can readily accept electrons directly transferred from the protein-bound NADH.

As compared with P450cam, these two properties, *i.e.*, the presence of the NADH binding site near the heme and the relatively strong NO binding to the ferric iron, are specific and unique to P450nor. For P450cam, there are no NADH binding sites in present and the iron-bound NO has an anionic character. The differences in these two properties are possibly responsible for the difference in the catalytic activity between NO reductase P450nor and monooxygenase P450cam.

Acknowledgment. We greatly thank Prof. S. S. Hasnain and Dr. R. W. Strange (Daresbury Laboratory, U.K.) for their helpful instruction of EXCURV92. This work was supported by the Biodesign Research Program from RIKEN, the MR Science Research Program in RIKEN, the SR Structural Biology Research Program in RIKEN, Special Coordination Funds from the Science and Technology Agency of Japan, and (to Y.S. and H.S.) the Grant-in-aid for Scientific Research on Priority Area from Ministry of Education.

JA9637816

(24) Usuda, K.; Toritsuka, N.; Matsuo, Y.; Kim, D.-H.; Shoun, H. *Appl. Environ. Microbiol.* **1995**, *61*, 883−889.